THE JOURNAL OF BIOLOGICAL CHEMISTRY VOL. 284, NO. 12, pp. 7914–7919, March 20, 2009
Printed in the U.S.A.

Insulin Regulates Fusion of GLUT4 Vesicles Independent of Exo70-mediated Tethering*[S]

Received for publication, August 20, 2008, and in revised form, December 23, 2008 Published, JBC Papers in Press, January 19, 2009, DOI 10.1074/jbc.M806460200

Vladimir A. Lizunov[‡], Ivonne Lisinski[§], Karin Stenkula[§], Joshua Zimmerberg[‡1], and Samuel W. Cushman[§]

From the [‡]Laboratory of Cellular and Molecular Biophysics, Program on Physical Biology, Eunice Kennedy Schriver National Institute of Child Health and Human Development, and the [§]Experimental Diabetes, Metabolism, and Nutrition Section, Diabetes Branch, NIDDK, National Institutes of Health, Bethesda, Maryland, 20892

Insulin regulates cellular glucose uptake by changing the amount of glucose transporter-4 (GLUT4) in the plasma membrane through stimulation of GLUT4 exocytosis. However, how the particular trafficking, tethering, and fusion steps are regulated by insulin is still debated. In a 3T3-L1 adipocyte cell line, the Exocyst complex and its Exo70 subunit were shown to critically affect GLUT4 exocytosis. Here we investigated the effects of Exo70 on tethering and fusion of GLUT4 vesicles in primary isolated rat adipose cells. We found that Exo70 wild type was sequestered away from the plasma membrane in non-stimulated cells, and its overexpression had no effect on GLUT4 trafficking. The addition of insulin increased the amount of Exo70 in the vicinity of the plasma membrane and stimulated the tethering and fusion of GLUT4 vesicles, but the rates of fusion and GLUT4 exposure were not affected by overexpression of Exo70. Surprisingly, the Exo70-N mutant induced insulin-independent tethering of GLUT4 vesicles, which, however, did not lead to fusion and exposure of GLUT4 at the plasma membrane. Upon insulin stimulation, the stationary pretethered GLUT4 vesicles in Exo70-N mutant cells underwent fusion without relocation. Taken together, our data suggest that fusion of GLUT4 vesicles is the rate-limiting step regulated by insulin downstream of Exo70-mediated tethering.

At the cellular level, glucose uptake is regulated by controlling the amount of the GLUT4 [2] glucose transporter present in the plasma membrane (1, 2). In insulin-responsive adipose and muscle cells, insulin regulates glucose uptake by promoting the exocytosis of specialized GLUT4 storage vesicles (GSV) (3–5). Although many steps of the insulin signal transduction pathway have been elucidated, the mechanism bridging insulin signaling with the actual fusion of GSV with the plasma membrane, with concomitantly enhanced glucose uptake, is still missing (6–8).

Increasing evidence suggests that insulin regulates GLUT4 exocytosis at many different levels such as intracellular sequestration of GLUT4 into GSV, traffic to the plasma membrane, and tethering and fusion (9, 10). Recent reports using total internal reflection fluorescence (TIRF) microscopy and comprehensive kinetic analysis using rat adipose cells and 3T3-L1 adipocytes suggest that both tethering and fusion of GSV are primary steps regulated by insulin stimulation (11–13).

Binding of insulin activates the insulin receptor tyrosine kinase, which mediates the signaling through a well established phosphatidylinositol 3-kinase-dependent pathway, and downstream activation of Akt that regulates GLUT4 trafficking, at least in part, through AS160 (14). Recent data suggest that AS160 is a negative regulator of Rabs and that through its GTPase-activating protein activity, it maintains the GLUT4 vesicles and associated Rabs in the state that excludes GSV from trafficking to the plasma membrane (15). A variety of evidence suggests the presence of a complementary pathway that acts not on GSV but rather activates the plasma membrane (16, 17). The activation of the plasma membrane might include the assembly of the tethering and docking machinery necessary for efficient and massive GSV exocytosis.

One of the most debated alternative pathways involves the Rho family member GTPase TC10 (18) that was shown to both target actin regulatory proteins neuronal Wiskott-Aldrich syndrome protein and Arp2/3, as well as recruit Exocyst components, to the plasma membrane (19). The Exocyst is a multisubunit complex involved in various exocytic pathways and has been proposed to tether vesicles to the plasma membrane and to mediate the interaction of fusion proteins (20–22). One of the core components of the Exocyst complex, the Exo70 kDa subunit, is critical for Exocyst complex assembly and has been shown to interact with the SNARE-associated protein Snapin (23). In yeast, Exo70 binds to the plasma membrane at the active site of exocytosis and targets specific secretory vesicles through interaction with the other Exocyst subunits associated with the vesicular membrane Sec5, Sec6, Sec8, Sec10, Sec15, and Exo84 (21). The truncated form of Exo70 lacking the C-terminal domain gets mislocalized in the yeast and results in the partial block of secretion (24). In 3T3L-1 cells, a similar mutant, Exo70-N (1–384 amino acids), exhibits a dominant-negative effect on GLUT4 exocytosis, suggesting that Exo70 is necessary for insulin-stimulated tethering of GLUT4 vesicles (18, 25). However, the role Exo70 plays in the insulin-stimulated tethering and fusion of GLUT4 vesicles remains unclear. In the current study, we utilized TIRF microscopy to visualize the traf-

* This work was supported, in whole or in part, by an National Institutes of Health grant through the Intramural Research Programs of the NICHD and NIDDK. The costs of publication of this article were defrayed in part by the payment of page charges. This article must therefore be hereby marked "*advertisement*" in accordance with 18 U.S.C. Section 1734 solely to indicate this fact.

[S] The on-line version of this article (available at http://www.jbc.org) contains a supplemental figure and four supplemental movies.

[1] To whom correspondence should be addressed. Tel.: 301-496-6571; Fax: 301-594-0813; E-mail: joshz@mail.nih.gov.

[2] The abbreviations used are: GLUT4, glucose transporter-4; GSV, GLUT4 storage vesicles; GFP, green fluorescent protein; HA, hemagglutinin; TIRF, total internal reflection fluorescence; SNARE, soluble NSF attachment protein receptors; NSF, *N*-ethylmaleimide-sensitive factor; WT, wild type.

ficking of GLUT4 vesicles in isolated rat adipose cells and tested the effects of Exo70 and its dominant-negative mutant (Exo70-N) on the tethering and fusion of GLUT4 vesicles.

EXPERIMENTAL PROCEDURES

Antibodies and Plasmids—Mouse anti-HA antibody (HA.11) was from Berkeley Antibody Co. (Richmond, CA). Anti-Myc antibody (9E10) was from Santa Cruz Biotechnology, Inc. (Santa Cruz, CA). Conjugated antibodies Rhodamine Red-X and Texas Red were from Jackson ImmunoResearch Laboratories Inc. (West Grove, PA). ^{125}I-sheep anti-mouse antibody was from Dupont. Myc-Exo70 and Myc-Exo70-N were kindly provided by Dr. A. R. Saltiel. Caveolin-GFP and tubulin-GFP were kindly provided by Dr. J. Lippincott-Schwartz. Construction of the HA-tagged GLUT4 has been described previously (26). To generate HA-GLUT4-mCherry, the mCherry was amplified from pRSET-B mCherry (gift from S. M. Simon) using the primers 5′-AGGTACCATGGTGAGCAAGG-3′ and 5′-AGCGGCCGCTTACTTGTAC-3′. The PCR product was cut with Kpn1 and Not1 and ligated into digested HA-GLUT4-GFP pQB125 to generate HA-GLUT4-mCherry pQB125. The sequence of HA-GLUT4-mCherry was verified by sequencing (MTR Scientific, Ijamsville, MD).

Cell Culture, Transfections, and Cell Surface Antibody Binding Assay—Preparation of isolated rat adipose cells from male rats (CD strain, Charles River Laboratories, MD), electroporation of rat adipose cells, and the cell surface antibody binding assay were performed as described (11, 27). Briefly, isolated adipose cells were electroporated (3 × 12 ms, 500 V/cm) with expression plasmids as indicated and cultured for 24 h at 37 °C in 5% CO_2. HA-GLUT4-GFP plasmid was used at a final concentration of 8 μg/ml; Myc-Exo70 and Myc-Exo70-N were also used at 8–16 μg/ml. After stimulation with 70 nM insulin for 30 min at 37 °C, subcellular trafficking of HA-tagged GLUT4 was stopped by the addition of 2 mM KCN, and the amount of the HA epitope on the cell surface was determined by an antibody binding assay using a monoclonal anti-HA antibody and a I^{125}-labeled sheep anti-mouse secondary antibody as described (27). Unless stated otherwise, the values obtained for empty vector-transfected cells were subtracted from all other values to correct for nonspecific antibody binding.

Immunostaining of Cells and Confocal Microscopy—Immunostaining of cells was performed as described elsewhere (3, 11). Cells were fixed in 4% paraformaldehyde/phosphate-buffered saline for 10 min at room temperature and then incubated for 2 h with primary antibodies followed by incubation with conjugated secondary antibodies for 1 h at room temperature. Immunostaining of cell surface HA was carried out under non-permeabilized conditions, whereas labeling of intracellular Exo70 was carried out in cells permeabilized by 0.1% saponin (Sigma). Secondary antibodies (Rhodamine Red-X and Texas Red) were imaged on an LSM510 confocal microscope (Carl Zeiss MicroImaging, Inc., NY) using planapochromat ×60 and ×100 1.4 NA oil objectives. A multitrack protocol with sequential excitation at 488- and 543-nm wavelengths was utilized to minimize cross-talk between the GFP and Rhodamine Red-X/Texas Red channels. For each experimental condition, 5–10 images/cell were recorded from 10–15 cells. For three-dimensional reconstruction, series of optical sections were collected at 0.5-μm intervals, with the pinhole set at one Airy disc.

TIRF Microscopy of Live Isolated Rat Adipose Cells—An objective-based total internal reflection microscopy setup built around an Olympus IX70 microscope was described previously (11). Transfected adipose cells that were incubated overnight were placed into Krebs-Ringer bicarbonate/Hepes buffer containing 5% bovine serum albumin and 5% Ficoll (Sigma) and added to Delta-T dishes (Bioptech, Butler, PA) kept at 37 °C. Where specified, cells were stimulated with 100 nM insulin. Cells floating in suspension were sandwiched between a dish coverslip and a second coverslip on top (22-mm round, No. 1., Erie Scientific, Portsmouth, NH). Series of 100–300 time lapse images for each cell were acquired at rates of 2–5 frames/s and streamed into Metamorph via a video A/D card (FlashBus).

Image Analysis—Stacks of time-lapse images were processed with ImageJ 1.37 (National Institutes of Health). Circular regions of 3-pixel radius were used to identify single GLUT4 vesicles according to the following criteria. (i) Mean pixel intensity was 20% higher than the background fluorescence, (ii) the pixel intensity profile had a local maximum, and (iii) the full width half-maximum of a Gaussian fit was less than 4 pixels. Vesicle traffic analysis was carried out as follows. Projection images with a maximum and mean intensity for each pixel were made for each stack representing 1 min of recording. The mean projection image was then subtracted pixel by pixel from the maximum projection to correct for non-uniform background and to exclude stationary objects. The resulting image contained the trajectories of mobile vesicles. Traces longer than 2 μm were identified visually, and the number of traces was counted for 2–3 regions (10 × 10 μm) for each cell. All data are represented as means ± S.D. unless stated otherwise.

RESULTS AND DISCUSSION

Expression and Subcellular Localization of GLUT4 and Exo70—To study the effect of Exo70 on GLUT4 exocytosis, we co-transfected isolated rat adipose cells with either Myc-tagged Exo70 wild type or Myc-tagged Exo70-N mutant (amino acids 1–384) and HA-GLUT4-GFP constructs. Confocal microscopy was used to assess the level of co-expression and visualize subcellular localization of both proteins. The percentage of cells expressing Myc-Exo70 (~30%) was slightly larger than that of cells expressing HA-GLUT4-GFP (~20%). However, more than 90% of the cells expressing HA-GLUT4-GFP also co-expressed Myc-Exo70, as was shown by anti-Myc antibody labeling (83 out of 92 cells in three independent experiments). No significant difference in co-expression was observed between wild-type and mutant Exo70.

Examination of confocal sections of the entire adipose cell showed that GLUT4 and Exo70 were localized to distinct structures that were scattered throughout the thin layer of cytoplasm between the plasma membrane and lipid droplet (Fig. 1*A*). Further, we examined the subcellular localization of GLUT4 and wild-type/mutant Exo70 in the vicinity of the plasma membrane. In non-stimulated cells, both GLUT4 and Exo70 had low plasma membrane staining, but substantial numbers of GLUT4 and Exo70 structures were close to the plasma membrane (within 0.5 μm) (Fig. 1*B*). Because we did not observe any co-

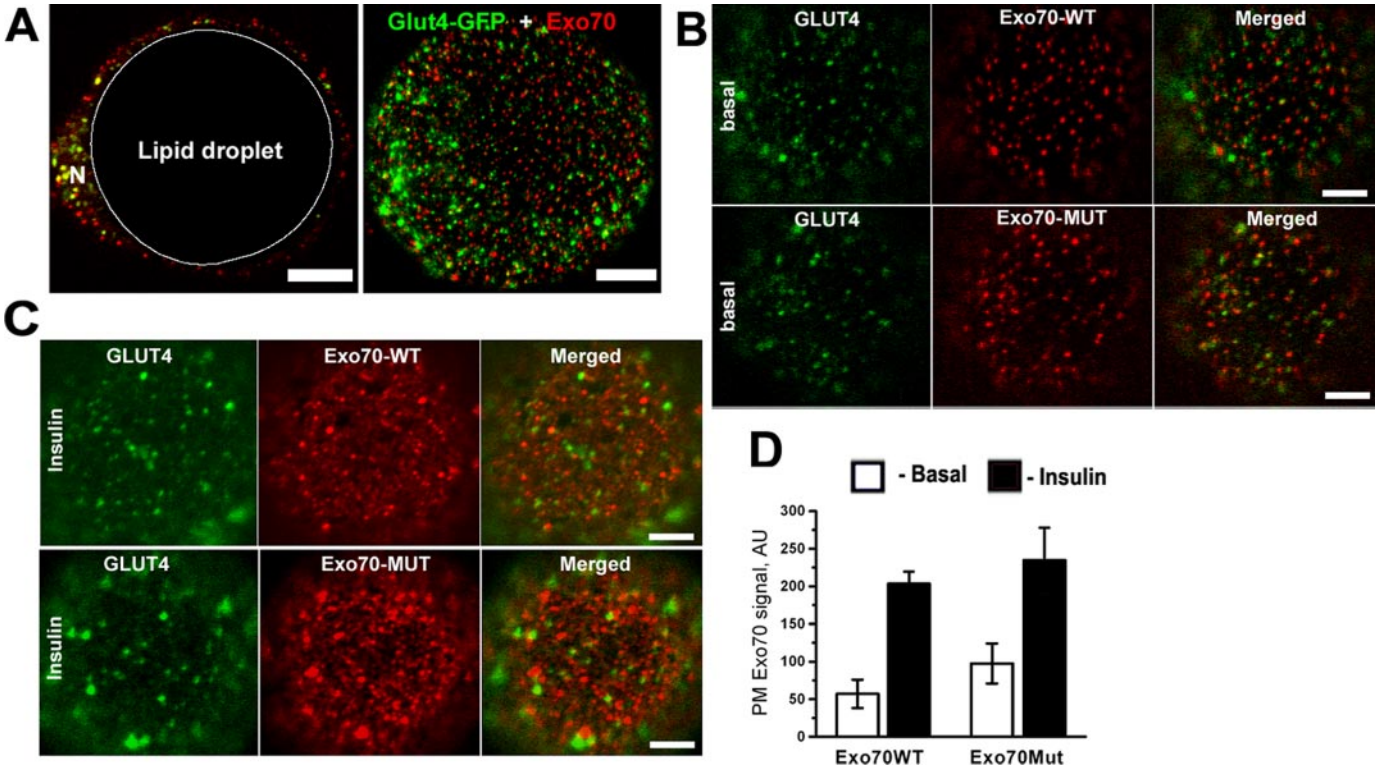

FIGURE 1. **Co-expression and subcellular localization, of GLUT4 and Exo70, in insulin-stimulated and nonstimulated (basal) isolated rat adipose cells.** *A*, confocal section of the center of the cell (*left*) and three-dimensional projection of the whole cell (*right*) in the basal state. Note the scattered distribution of GLUT4 and Exo70 throughout the thin layer of cytoplasm surrounding the lipid droplet. *N*, nucleus. *B* and *C*, confocal section of the plasma membrane region of the basal (*B*) and insulin-stimulated (*C*) cells. GLUT4 is shown in *green*, and Myc-Exo70 is shown in *red*. Cells were transfected with HA-GLUT4-GFP and Myc-Exo70WT (*upper panels*) or Myc-Exo70-N mutant (*Exo70-MUT*) (*lower panels*). Cells were either kept basal or stimulated with 67 nM insulin for 15 min, fixed, permeabilized, and stained with anti-Myc-antibody followed by Rhodamine Red-X-conjugated antibody. All *bars*, 10 μm. *D*, quantified fluorescence of the Myc antibody at the plasma membrane. *AU*, arbitrary units.

localization between GLUT4 and Exo70 puncta, we suggest that the majority of Exo70 is associated with vesicular compartments distinct from GLUT4 vesicles. Although GLUT4 is known to localize in GSV in the basal state and redistribute to the plasma membrane upon insulin stimulation, Exo70 is considered to be a cytosolic protein that has not been reported to associate with intracellular vesicles. Thus, we expected it to have a diffuse rather than punctate staining. To confirm the punctate distribution of Exo70, we also used an antibody directed to Exo70 that showed the same pattern (data not shown).

Insulin stimulation induced a significant redistribution of GLUT4 and both wild-type and mutant Exo70 to the plasma membrane (Fig. 1*C*). This led to an effective increase in the overlap of GLUT4 and Exo70. However, the GSV and Exo70 puncta still did not co-localize. Although the diffuse GLUT4 staining represents GLUT4 inserted into the plasma membrane, the diffuse Exo70 staining is probably due to increased association with the plasma membrane leaflet. (Fig. 1*D*). This conforms to similar findings in 3T3-L1 adipocytes. As a part of the Exocyst complex, Exo70 is expected to only transiently interact with GLUT4 vesicles at the plasma membrane to mediate their tethering. Thus, low association of GLUT4 with Exo70 in the absence of insulin correlates with the low rate of GSV tethering and fusion reported previously for non-stimulated cells. Moreover, the increased overlap of Exo70 and GLUT4 upon insulin stimulation further supports the involvement of Exo70 in the tethering of GSV. However, in contrast to published 3T3-L1 cell data (19, 25), we could not detect a significant difference in redistribution between wild-type and mutant Exo70 in response to insulin.

Effect of Exo70 on GLUT4 Vesicle Tethering—To test how Exo70 affects tethering of GLUT4 vesicles, we quantified trafficking of GSV in the vicinity of the plasma membrane of isolated adipose cells using total internal reflection fluorescence microscopy. Consistent with previous reports, GSV traffic was supported by the microtubule network, and all detected long range movement of GSV was along microtubules (Fig. 2*A*). The traffic intensity was measured as the number of trafficking GSV per defined area of 10 $\times$ 10 μm/min. Under non-stimulated conditions, cells expressing wild-type Exo70 exhibited intensive GLUT4 vesicle trafficking, similar to control cells expressing only GLUT4-GFP. Projections of traces (Fig. 2*B*) illustrate the traffic intensity as traces/100 μm^2/min. However, although cells expressing wild-type Exo70 showed traffic intensity similar to control cells (GLUT4-GFP only), cells expressing Exo70-N mutant exhibited a significantly reduced GSV traffic (Fig. 2, *B* and *C*). This suggests that the Exo70-N mutant might induce GSV tethering, mimicking the effect of insulin. Consistent with previous findings, insulin stimulation decreased GSV traffic in control cells and cells expressing wild-type Exo70 by increasing the frequency of vesicle tethering to the plasma membrane (Fig. 2*C*). However, insulin did not induce any further decrease of GSV trafficking in cells expressing Exo70

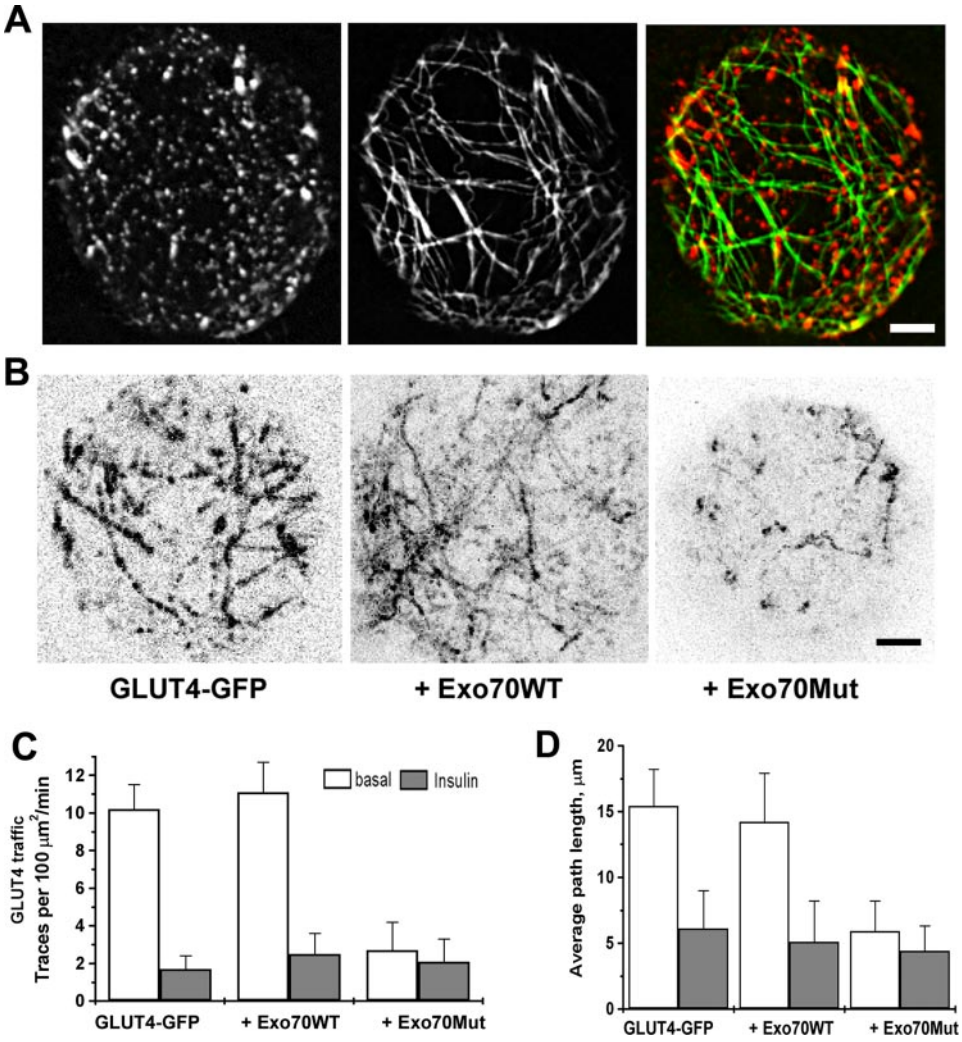

FIGURE 2. **Traffic of GLUT4 vesicles in Exo70-WT and Exo70-N mutant (*Exo70MUT*) cells visualized by total-internal reflection fluorescence microscopy.** *A*, GLUT4-mCherry vesicle (*red*) and tubulin-GFP (*green*) in the TIRF zone of Exo70-N-expressing cell. Note the intact microtubular network. *B*, projection images mapping traces of trafficking GLUT4 vesicles in the basal state in control cells and cells expressing Exo70-WT and Exo70-N mutant. Images are inverted for clarity. All *bars*, 5 μm. *C*, quantified traffic intensity (traces/100 μm^2/min). *D*, average path length of GLUT4 vesicles exhibiting movement in the TIRF zone.

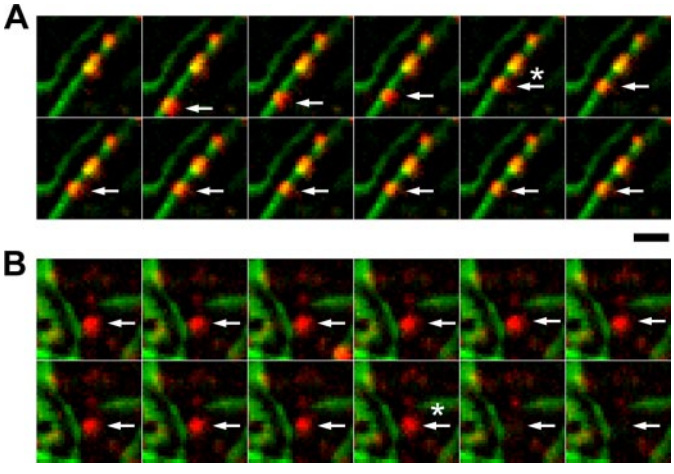

FIGURE 3. **Tethering and fusion events of GLUT4 vesicles in cells expressing Exo70-N mutant.** *A*, frames of time-lapse recording showing tethering event of GLUT4 vesicle in non-stimulated cell. *B*, frames of time-lapse recording showing insulin-stimulated fusion of pretethered vesicles. *Red*, GLUT4-mCherry vesicle; *green*, tubulin-GFP. *Bar*, 1 μm.

mutant (Fig. 2*C*). This suggests that the effect of insulin on tethering of GSV can be mediated through interactions dependent on the truncated part of Exo70.

The decreased GSV trafficking intensity in the Exo70 mutant cells was not due to adverse effects on the microtubules, as we found the microtubule network intact (Fig. 1*A*), with the density and length of microtubules similar to control cells (supplemental material). Although the expression of Exo70 mutant diminished the path length of mobile GLUT4 vesicles (Fig. 2*D*), the speed was unaffected ($\sim$1.7 $\pm$ 0.5 μm/s, calculated for long tracks $>$5 μm). Also, to address the specificity of the Exo70 mutant effect on GSV traffic, we co-expressed it with caveolin-GFP and found no effect on the traffic of caveolin-labeled vesicles (supplemental material). Altogether, these data indicate that the effect of the Exo70 mutant is not related to the molecular motors involved in microtubule-based traffic but rather to the probability of GSV tethering. In contrast to insulin-induced tethering of GSV, which was followed shortly by fusion events, the Exo70 mutant-induced GSV tethering did not lead to fusion in the absence of insulin (Fig. 3*A*). The addition of insulin was required to induce fusion of pretethered GSV in Exo70 mutant-expressing cells (Fig. 3*B*). This further supports the notion that insulin is necessary for stimulating the fusion step of GSV exocytosis.

Effect of Exo70 on GLUT4 Vesicle Fusion—To test how Exo70 affects fusion of GSV, we utilized an HA-GLUT4-GFP construct. This allows detection of GLUT4 inserted into the plasma membrane exposing the HA epitope to the exterior by the binding of an HA antibody in non-permeabilized cells (27). The amount of GLUT4 in the plasma membrane was assessed in isolated rat adipose cells co-expressing HA-GLUT4-GFP and either wild-type Myc-Exo70 or mutant Myc-Exo70. The level of HA exposure was measured in bulk using a radioactive secondary antibody. In control experiments, co-localization of HA labeling with GFP fluorescence was assessed (Fig. 4, *A* and *B*) to visualize both the exposed and the intracellular GLUT4. In non-stimulated cells, the amount of GLUT4 inserted into the plasma membrane was low ($<$30% when compared with insulin), and most of the HA antibody labeling was localized to puncta (Fig. 4, *A* and *B*, *upper panels*). These puncta can represent the rare kiss-and-run fusion events of GSV (12) or sites of

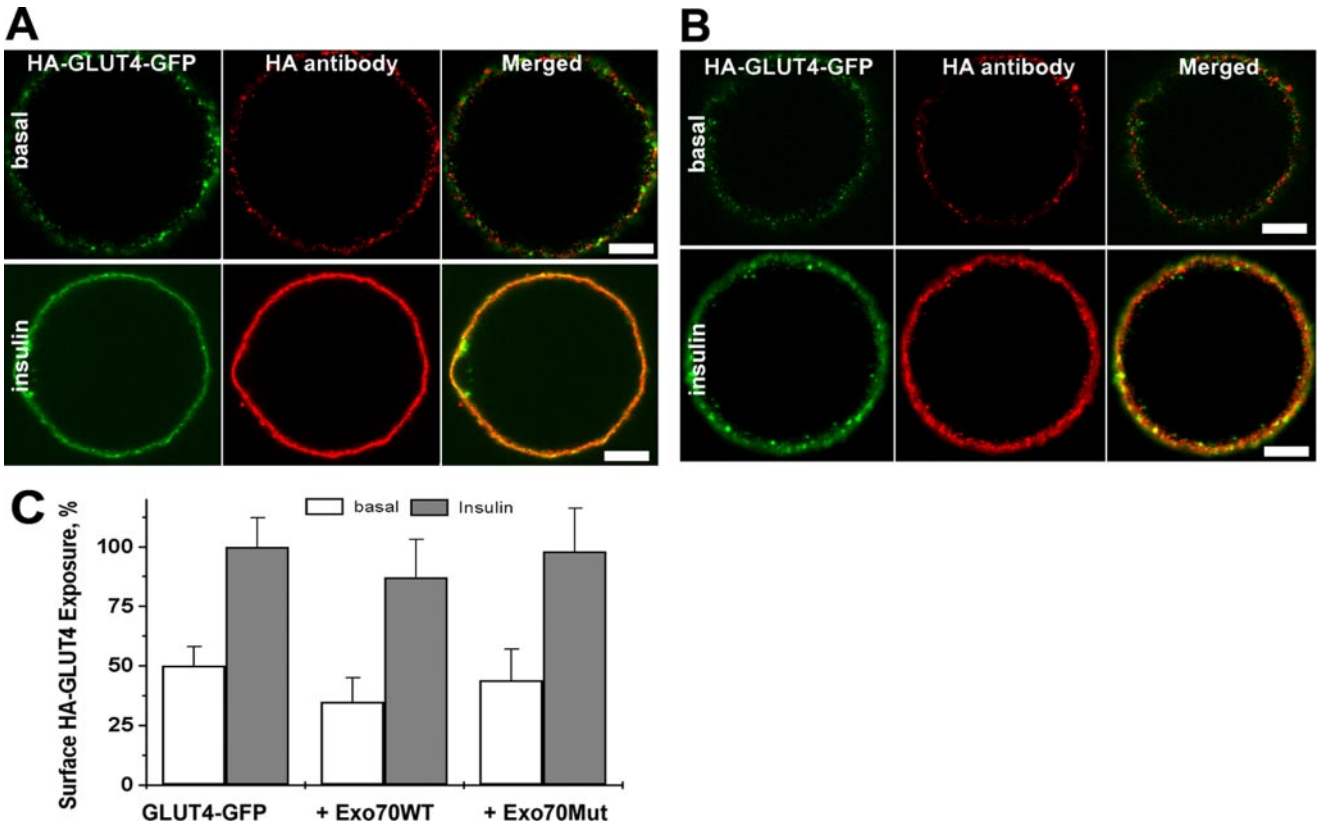

FIGURE 4. **Insulin-induced exposure of GLUT4 at the plasma membrane of Exo70-WT and Exo70-N mutant (*Exo70MUT*) cells.** *A* and *B*, confocal images of isolated adipose cells transfected with WT Exo70 (*A*) or mutant Exo70-N (*B*). HA-GLUT4-GFP is shown in *green*; GLUT4 with HA epitope exposed at the plasma membrane surface is shown in *red*. Cells were kept basal (*upper panels*) or stimulated with 67 nM insulin for 15 min (*lower panels*), fixed without permeabilization, and stained with mouse anti-HA-antibody followed by anti-mouse Rhodamine Red-X antibody. Note the difference between the punctuate localization of GLUT4 throughout the thin layer of cytoplasm in the basal state and the diffuse plasma membrane staining in the insulin-stimulated state. All *bars*, 10 μm. *C*, the relative amount of the HA epitope on the cell surface determined by an antibody-binding assay using a monoclonal anti-HA antibody and a ^{125}I-labeled sheep anti-mouse secondary antibody.

GLUT4 clustering at endocytic pits (13). After insulin stimulation, both Exo70 WT and Exo70 mutant cells exhibited a similar 2–3-fold increase in HA-antibody binding (Fig. 4*C*, *solid bars*) and showed diffuse staining of the plasma membrane that colocalized with the GLUT4-GFP signal (Fig. 4, *A* and *B*, *lower panels*). We could not detect any difference in distribution or insertion of GLUT4 between control cells and cells expressing either Exo70 wild type or Exo70 mutant. Thus, we conclude that the overall rate of GLUT4 exocytosis is not affected by expression of wild-type or mutant Exo70. The absence of correlation between GLUT4 insertion and increased GSV tethering suggests that tethering is not the rate-limiting step.

Different Effects of Exo70 in 3T3-L1 Cells and Primary Adipose Cells—Insulin regulates GLUT4 exocytosis at multiple steps involving trafficking, tethering, and fusion. The molecular events associated with stimulated GLUT4 exocytosis are likely to take place at both the vesicular surface and the plasma membrane. In the current study, we investigated the role of the Exocyst component Exo70 on the trafficking and tethering events of GSVs. We did not see any effect of overexpressing the wild-type Exo70 protein. Surprisingly, the Exo70-N mutant, reported to block the assembly of the Exocyst complex and GLUT4 exocytosis in differentiated 3T3-L1 cells, enhances the tethering in the primary adipose cells but does not affect the rate of fusion, neither in the basal nor in the insulin-stimulated state. The effect of the Exo70 mutant on the tethering in basal conditions was strikingly similar to insulin-induced tethering but is insufficient to induce fusion. This fact indicates that insulin regulates fusion steps of GLUT4 exocytosis independently of upstream tethering where Exo70 might be involved.

The mechanism of Exo70 targeting to the sites of exocytosis at the plasma membrane remains controversial. Recent data from budding yeast studies suggest that the C-terminal domain of Exo70 protein is important for specific binding to phosphatidylinositol 4,5-bisphosphate lipids (24). Because insulin is known to stimulate generation of phosphatidylinositols, it can serve as means of Exo70 recruitment to the plasma membrane (18). On the other hand, the N-terminal domain of Exo70 (1–99 amino acids) binds TC10 and Snapin (23) and thus can associate with SNARE machinery through protein interaction without relying on lipid binding.

In non-stimulated 3T3-L1 cells, Exo70 is located in the perinuclear regions (18, 19). In response to insulin, the Exo70 wild type translocates to the plasma membrane, whereas the Exo70-N mutant stays in the perinuclear region (19). This was thought to disrupt assembly of the Exocyst complex at the plasma membrane and ablate the GLUT4 exocytosis. In the mature primary adipose cells, we found that both wild-type and mutant Exo70 were localized in the TIRF zone within 200 nm of the plasma membrane and not in the perinuclear region as in

the basal 3T3L-1 differentiated adipocytes. Thus, there is no need for long ranged translocation/movement of Exo70 necessary for GLUT4 exocytosis in mature adipose cells.

In fact, this discrepancy in distribution is not specific to Exo70 but rather is a general difference in cellular architecture between newly differentiated 3T3-L1 adipose cells and mature primary adipose cells (3, 27). For example, in primary adipocytes, 90% of the GLUT4 resides in GSV close to the plasma membrane surface and does not require translocation from the perinuclear areas in response to insulin (11). The central lipid droplet in primary adipose cells occupies 99% of the cell volume and thereby pushes all the intracellular compartments to the periphery in close apposition to the plasma membrane. Even the Golgi structures are found to be dispersed far away from the nucleus. This unique architecture of mature adipose cells may promote a shift to local autonomous recycling of GLUT4 to minimize its dependence on recycling compartments located in perinuclear area.

So far, most studies addressing the molecular mechanisms of insulin-regulated GLUT4 exocytosis have been done using cultured adipose cells, 3T3-L1 cells, and isolated primary cells, models that both have disadvantages. Although the differentiated 3T3-L1 cells never develop into fully mature adipose cells and are maintained in culture only for a relatively short period after differentiation, mature adipose cells can be cultured only for a few days after isolation, which limits the application of techniques such as small interfering RNA. New strategies involving stromal cells derived from adipose tissue have shown a potential to develop into mature adipose cells that could be kept in culture without losing the adipose phenotype (28). This promises to be an invaluable tool for answering the question how differentiation and maturation of adipocytes affects molecular machinery involved in GLUT4 exocytosis.

REFERENCES

1. Cushman, S. W., and Wardzala, L. J. (1980) *J. Biol. Chem.* **255,** 4758–4762
2. Suzuki, K., and Kono, T. (1980) *Proc. Natl. Acad. Sci. U. S. A.* **77,** 2542–2545
3. Malide, D., Dwyer, N. K., Blanchette-Mackie, E. J., and Cushman, S. W. (1997) *J. Histochem. Cytochem.* **45,** 1083–1096
4. Rea, S., and James, D. E. (1997) *Diabetes* **46,** 1667–1677
5. Bryant, N. J., Govers, R., and James, D. E. (2002) *Nat. Rev. Mol. Cell Biol.* **3,** 267–277
6. Saltiel, A. R., and Pessin, J. E. (2003) *Traffic* **4,** 711–716
7. Williams, D., and Pessin, J. E. (2008) *J. Cell Biol.* **180,** 375–387
8. Lodhi, I. J., Chiang, S. H., Chang, L., Vollenweider, D., Watson, R. T., Inoue, M., Pessin, J. E., and Saltiel, A. R. (2007) *Cell Metab.* **5,** 59–72
9. Sparling, D. P., Griesel, B. A., Weems, J., and Olson, A. L. (2008) *J. Biol. Chem.* **283,** 7429–7437
10. Zaid, H., Antonescu, C. N., Randhawa, V. K., and Klip, A. (2008) *Biochem. J.* **413,** 201–215
11. Lizunov, V. A., Matsumoto, H., Zimmerberg, J., Cushman, S. W., and Frolov, V. A. (2005) *J. Cell Biol.* **169,** 481–489
12. Bai, L., Wang, Y., Fan, J., Chen, Y., Ji, W., Qu, A., Xu, P., James, D. E., and Xu, T. (2007) *Cell Metab.* **5,** 47–57
13. Huang, S., Lifshitz, L. M., Jones, C., Bellve, K. D., Standley, C., Fonseca, S., Corvera, S., Fogarty, K. E., and Czech, M. P. (2007) *Mol. Cell Biol.* **27,** 3456–3469
14. Mîinea, C. P., Sano, H., Kane, S., Sano, E., Fukuda, M., Peränen, J., Lane, W. S., and Lienhard, G. E. (2005) *Biochem. J.* **391,** 87–93
15. Sano, H., Eguez, L., Teruel, M. N., Fukuda, M., Chuang, T. D., Chavez, J. A., Lienhard, G. E., and McGraw, T. E. (2007) *Cell Metab.* **5,** 293–303
16. Koumanov, F., Jin, B., Yang, J., and Holman, G. D. (2005) *Cell Metab.* **2,** 179–189
17. Baumann, C. A., Ribon, V., Kanzaki, M., Thurmond, D. C., Mora, S., Shigematsu, S., Bickel, P. E., Pessin, J. E., and Saltiel, A. R. (2000) *Nature* **407,** 202–207
18. Jiang, Z. Y., Chawla, A., Bose, A., Way, M., and Czech, M. P. (2002) *J. Biol. Chem.* **277,** 509–515
19. Inoue, M., Chang, L., Hwang, J., Chiang, S. H., and Saltiel, A. R. (2003) *Nature* **422,** 629–633
20. TerBush, D. R., Maurice, T., Roth, D., and Novick, P. (1996) *EMBO J.* **15,** 6483–6494
21. Boyd, C., Hughes, T., Pypaert, M., and Novick, P. (2004) *J. Cell Biol.* **167,** 889–901
22. Hsu, S. C., Hazuka, C. D., Foletti, D. L., and Scheller, R. H. (1999). *Trends Cell Biol.* **9**, 150–153
23. Bao, Y., Lopez, J. A., James, D. E., and Hunziker, W. (2008) *J. Biol. Chem.* **283,** 324–331
24. He, B., Xi, F., Zhang, X., Zhang, J., and Guo, W. (2007) *EMBO J.* **26,** 4053–4065
25. Ewart, M. A., Clarke, M., Kane, S., Chamberlain, L. H., and Gould, G. W. (2005) *J. Biol. Chem.* **280,** 3812–3816
26. Quon, M. J., Guerre-Millo, M., Zarnowski, M. J., Butte, A. J., Em, M., Cushman, S. W., and Taylor, S. I. (1994) *Proc. Natl. Acad. Sci. U. S. A.* **91,** 5587–5591
27. Al-Hasani, H., Hinck, C. S., and Cushman, S. W. (1998) *J. Biol. Chem.* **273,** 17504–17510
28. Vermette, M., Trottier, V., Menard, V., Saint-Pierre, L., Roy, A., and Fradette, J. (2007) *Biomaterials* **28,** 2850–2860